atmosphere

Article

Examining the Effects of Tree Canopy Coverage on Human Thermal Comfort and Heat Dynamics in Courtyards: A Case Study in Hot-Humid Regions

Chang Lin [1], Jiahao Yang [2], Jun Huang [1] and Ruize Zhong [1,*]

[1] School of Visual Arts Design, Guangzhou Academy of Fine Arts, Guangzhou 510261, China; linchang@gzarts.edu.cn (C.L.)
[2] School of Architectrue and Urban Planning, Guangzhou University, Guangzhou 510006, China
* Correspondence: zrz@gzarts.edu.cn

Abstract: Providing thermal comfort in the courtyards of academic buildings is important and increasing tree canopy coverage (TCC) presents a convenient and feasible method to achieve this; however, few studies have comprehensively evaluated the cooling effects of TCC, considering both outdoor thermal comfort and heat dynamics. In this study, we selected two typical academic buildings at Guangzhou University, each with courtyards having different height-to-width ratios (H/W ratios). We employed both field measurements and ENVI-met-based numerical models to simulate scenarios with varying TCCs. The results demonstrated that the cooling effects caused by arranging trees increase with the TCC values. During the hottest hours of the day, trees arranged in courtyards with high H/W ratios exhibited a superior cooling effect compared to those in courtyards with low H/W ratios, with a difference of up to 0.6 °C in the PET (physiological equivalent temperature); however, over the entire daytime, the total sensible heat reduction achieved by trees in courtyards with low H/W ratios surpassed that of courtyards with high H/W ratios, with a difference of up to 0.25×10^4 J/m^2. Our findings underscore the crucial role of TCC in enhancing cooling in the courtyard of academic buildings, with important implications for university planning and design.

Keywords: tree canopy coverage; outdoor thermal comfort; sensible heat dynamic; courtyard; hot-humid regions

check for updates

Citation: Lin, C.; Yang, J.; Huang, J.; Zhong, R. Examining the Effects of Tree Canopy Coverage on Human Thermal Comfort and Heat Dynamics in Courtyards: A Case Study in Hot-Humid Regions. *Atmosphere* **2023**, *14*, 1389. https://doi.org/10.3390/atmos14091389

Academic Editor: Teodoro Georgiadis

Received: 10 August 2023
Revised: 26 August 2023
Accepted: 31 August 2023
Published: 2 September 2023

1. Introduction

In recent years, rapid urbanization and the impacts of climate change have intensified the urban heat island (UHI) effect in dense cities. Urban heat islands refer to urban areas with higher temperatures than the surrounding rural areas, leading to more frequent occurrences of extreme weather conditions [1,2]. Exposure to extreme heat environments can pose severe threats to human health and well-being [3–5]. Consequently, high temperatures encourage people to spend more time indoors, relying on artificial air conditioning to achieve comfort [6,7]; however, this growing trend contributes to a sedentary lifestyle, negatively impacting human health and significantly increasing building energy consumption [8–10]. Therefore, addressing this issue requires prioritizing the design for urban climate resilience, a crucial aspect to reduce carbon emissions and enhance urban livability [11,12].

Among the various mitigation strategies aimed at achieving resilient urban design, the most extensively studied perspectives in the literature include the utilization of urban geometry [13,14], shading [15,16], greenery [17,18], and reflective technologies [19,20]. Another highly effective strategy for mitigating the UHI effect is the implementation of courtyards as "Urban Cool Islands" [21]. Courtyards have been widely adopted in different climatic regions, particularly in hot and arid climates and temperate climate zones, as well as in cold regions and hot-humid regions. The advantages of courtyards for such diverse climates are noteworthy; they create more shading in hot climates, enhance natural ventilation in humid climates, and provide protection against cold winds in temperate and cold climates [22].

Buildings and trees play crucial roles in determining the human thermal comfort of courtyards, as they collectively influence the redistribution of the occupant thermal sensations in outdoor spaces. Buildings provide shade, effectively preventing the surface from heating up due to solar radiation [23]. Additionally, the arrangement and form of buildings impact the air flow, facilitating heat dispersion [24]. Many design measures have been proposed to enhance the outdoor thermal comfort of courtyards. Eduardo Diz-Mellado et al. discovered that when the aspect ratio (AR) of a courtyard exceeds three, the comfort level is achieved for 90–100% of the day's hours, and when the AR is between two and three, it reaches approximately 70–80%. Moreover, the cooling requirements of courtyards vary significantly based on their AR, with differences of up to 18% [25,26]. Similarly, Nazanin Nasrollahi et al. found that courtyards with high height-to-width (H/W) ratios and a southward orientation offered better shading during summer while permitting solar radiation in and regulating the wind speed during winter [27]. This finding aligns with the research of Rodriguez-Algeciras, Jose, et al., which suggests that orienting a courtyard's long axis away from the east to west direction results in a lower level of T_{mrt} (mean radiant temperature) in the summer [28].

Furthermore, trees not only regulate the outdoor microclimate through shading, by absorbing and reflecting solar radiation, but they also regulate the environmental conditions through transpiration. Previous studies have investigated and generally confirmed the cooling effects of trees on the city to the neighborhood scales. For instance, Jin et al. conducted a study demonstrating that increasing the number of trees in an open space by threefold of the advisory guidelines led to a significant reduction of the average air temperature by 0.9 °C, the mean radiant temperature by 11.0 °C, the physiological equivalent temperature by 4.5 °C, and the wind speed by 0.30 m/s [29]. In another study, Zhao et al. found that at 15:00 hours, trees arranged along a street can provide a cooling effect of 1–1.5 °C (PET) to the human body at the pedestrian level. Although adjusting the position of the trees may cause a slight loss in the air temperature cooling effect of 0.05 °C, this can still achieve a T_{mrt} cooling effect of 0.1 °C, which is three times the temperature cooling effect [30]. Furthermore, Zhang et al. discovered that planting trees in courtyards can reduce the PET by 20.0 °C and decrease the cooling demand by approximately 2.6% [31]; however, these studies primarily focused on microclimatic parameters, including the air temperature (T_a), relative humidity (RH), globe temperature (T_g), and wind speed (V_a).

Heat fluxes of urban landscapes exhibit variation at different times and seasons, and these energy dynamics significantly affect the thermal comfort of urban residents [32]. For example, Li et al. found that tree evapotranspiration and enhanced hydrological processes in different urban land use types in Singapore led to varying increases in the latent heat flux and reductions in the sensible heat flux [33]. Another study by Heusinger, Jannik et al. revealed that the difference in the urban excess heat reduction between green roofs and common roofs can be as high as 3% [34]. Furthermore, the aspect ratio and building height also exert notable effects on local energy fluxes. For instance, at noon, increasing the aspect ratio from 0.5 to 10.0 can result in a reduction of 300.0 W/m^2 in the sensible heat flux [35,36]; therefore, it is essential to adopt comprehensive methods to evaluate the cooling capacity of thermal mitigation strategies, including tree arrangements in courtyards. The microclimate simulation software, ENVI-met, provides the possibility to achieve this goal. ENVI-met is a three-dimensional microclimate computational fluid dynamics (CFD) software capable of simulating microscale interactions within built environments. It provides physical quantities such as the T_a, RH, V_a, and T_{mrt} [37,38]. Moreover, ENVI-met is able to simulate the effects of detailed vegetation, making it widely used for microclimate simulation in urban spaces, especially in hot-humid regions [39,40], which aligns well with the objectives of this research [41,42].

Therefore, in this study, we aim to address the above-mentioned insufficiency by utilizing the human thermal comfort index and the total sensible heat change to evaluate the cooling efficiency provided by TCC in academic building courtyards with different W/L ratios. The evaluation was conducted under typical summer climate conditions in hot-humid areas. Furthermore, based on our findings, we propose recommendations for the construction and renovation of courtyards in academic buildings.

2. Materials and Methods

2.1. Climate Conditions

Guangzhou (23°12′ N; 113°20′ E), the capital of Guangdong Province, is located on the subtropical coast of China. It experiences a monsoon-influenced humid subtropical climate, characterized by hot and humid summers, abundant rainfall, and relatively temperate and dry winters. The annual mean temperature and humidity are 22.0 °C and 77% [43], respectively. July is the hottest month, with an average temperature of 28.7 °C. The prevailing wind directions in Guangzhou exhibit seasonality. During the summer, south-easterly winds dominate due to the influence of subtropical highs and the South China Sea lows.

2.2. Study Area and Field Measurement

As shown in Figure 1, we selected two adjacent academic buildings of Guangzhou University as the research object, of which the academic building on the east side was named DZXX, and the academic building on the west side was named LX. These academic buildings are similar in size, with both having a height of 24 m and a total of 7 floors, with the ground floors serving as overhead spaces. Their difference is the H/W ratio of their respective courtyards. Among them, the courtyard of DZXX has a height of 24 m and a width of 27 m, while the courtyard of LX has a height of 24 m and a width of 33 m; therefore, their H/W are defined as 0.9 and 0.7, respectively. To evaluate the thermal environment and verify the accuracy of the simulation model, we conducted field measurements on 21 July 2022. Previous studies have shown that low airflow velocity and high radiation load conditions may have a significant impact on the accuracy of some measurement instruments' results [44,45]; therefore, in this study, a total of 5 measurement points were distributed in the overhead space of two academic buildings, avoiding direct sunlight measurement instruments. The overhead space refers to the bottom floor of a building, which is completely open and has no walls or windows [46]. Each measurement point was set at 1.5 m above ground. The measurement instruments and their respective parameters used for the field measurements are listed in Table 1. Among them, the globe thermometer (JTR 04) used was 150 mm in diameter with an emissivity equal to 0.95.

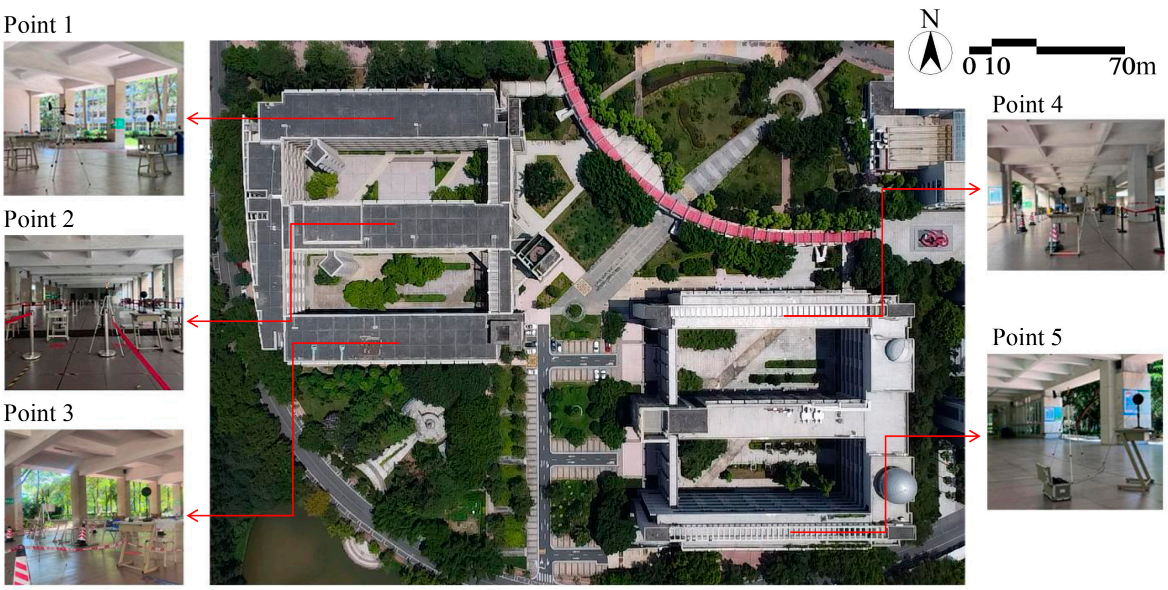

Figure 1. The field survey in this research.

Table 1. Measuring instruments for the numerical model validation.

Instrument	Parameter	Measuring Range	Accuracy
HOBO Pro	Air temperature	–40.0 to 70.0 °C	±0.5 °C
HOBO Pro	Relative humidity	0 to 100%	±2.5%
Kestrel5500	Wind speed	0 to 5 m·s^{-1}	±0.05 m·s^{-1}
JTR04	Black bulb temperature	10.0 to 85.0 °C	±0.5 °C

2.3. Model Validation

The validation of the ENVI-met model is vital to ensure reliable simulation outputs [47]. In many previous studies, the reliability of the ENVI-met model output was assessed by comparing it with the measured T_a and RH [48–50]; therefore, the air temperature and RH of each point were measured on-site and compared with the simulated values of the ENVI-met model. Subsequently, the model reliability was assessed. The correlation coefficients (R^2), mean absolute error (MAE), and root mean square error ($RMSE$) were used to test the model accuracy [51], as calculated using Equations (1)–(3):

$$RMSE = \sqrt{\frac{\sum_{i=1}^{n}(X_{obs,i} - X_{model,i})^2}{n}} \tag{1}$$

$$MAE = \frac{\sum_{i=1}^{n}\left|X_{obs,i} - X_{model,i}\right|}{n} \tag{2}$$

$$R^2 = 1 - \frac{\sum_{i=1}^{n}(X_{obs,i} - X_{model,i})^2}{\sum_{i=1}^{n}\left(X_{obs,i} - X_{obs}\right)^2} \tag{3}$$

where X_{obs} is the measured value, X_{model} is the simulated value, and n is the number of data values.

2.4. Case Studies

In this study, two models were constructed according to the current situation. In both models, the height of the building was 24 m tall, with ordinary concrete vertical walls and a flat roof. The underlying surface was mainly composed of asphalt and red bricks. In addition, trees surrounding the buildings have also been established. The main difference between the two models was the H/W ratio of the academic building, which was 0.9 (DZXX) and 0.7 (LX), respectively. The input parameter settings for the ENVI-met model are presented in Table 2. The geographical location coordinates were set to 113.20 °E and 23.12 °N, and the time zone was set to UTC/GMT + 08:00. This model accurately reproduced the building where the test site was located as well as the surrounding greenery. The wind speed, hourly temperature and humidity data were derived from data recorded by meteorological stations. The weather station used in this study was the HOBO meteorological station, which was shielded by ventilated boxes to avoid direct sunlight. The meteorological station was located on the roof of the academic building on the north side of the DZXX, with a distance of approximately 100 m. Solar radiation data were calculated using the geographic location data system input into the ENVI-met model, and the solar radiation correction ratio input was 1.0 [50].

Table 2. ENVI-met input parameters for the simulations.

Variable	Settings
Size and resolution	51 × 48 × 20 x = 3 m, Y = 3 m, and Z = 3 m
Date	21 July 2022
Duration	7:00 a.m.–18:00 p.m.
Solar radiation correction ratio	1.0
Initial T_a and RH	29.3 °C/79.1%
Wind velocity and wind direction at 10 m	1.1 m/s, 135°
Specific humidity at 2500 m	10.76 g/kg
Soil initial temperature	31.5 °C (0–20 cm)/33.9 °C (20–50 cm)/32.9 °C (<50 cm)
Soil initial humidity	30% (0–20 cm)/40% (20–50 cm)/50% (<50 cm)
Albedo	Wall: 0.30 Roof: 0.45 Asphalt: 0.20 Brick road: 0.30

During the field investigation, the surrounding vegetation type was determined to be *Michelia able.* To ensure a more precise prediction of the tree canopy coverage's impact on the thermal environments of courtyards with different H/W ratios, a specific ENVI-met model of *Michelia able* was established for subsequent simulations. The model parameters of *Michelia able* were set as follows: a tree height of 10.46 m, crown diameter of 6 m, under-branch height of 3 m, and leaf area index (LAI) value of 2.46 m^2/m^2 [52]. The trees were planted 6 m away from the academic buildings. Considering the uniform distribution of tress in each courtyard, six TCC scenarios were implemented for each courtyard, with percentages of 21%, 26%, 31%, 36%, 47%, and 68%, respectively. Additionally, a 0% scenario was included, representing the absence of greenery inside each courtyard, serving as a control.

2.5. Thermal Comfort Assessment Indices

Many thermal comfort indices derived from the human energy balance have been developed to evaluate the outdoor environment, such as the wet-bulb globe temperature (WBGT), physiological equivalent temperature (PET), and the universal thermal climate index (UTCI) [53,54]. Among them, the PET is determined using the Munich energy balance model for individuals (MEMI) [55]. It represents the equivalent air temperature in a typical indoor condition and approximates the human body's thermal perceptions in an outdoor setting [56]. Meanwhile, independent physiological parameters, such as height, age, and the human metabolic rate of activity, were considered for calculating the PET index [57]. Furthermore, the PET is one of the most widely used thermal indices for assessing thermal comfort in degrees Celsius (°C) and it has been adopted in numerous studies and practical applications [40,58–60]; therefore, we selected the PET as the evaluation index to measure the thermal environments of the courtyards in the academic buildings. It is worth noting that the thermal comfort perception can vary across different regions. For instance, Lai et al. pointed out that residents in the north are more receptive to cold environments compared to in Europe and Taiwan [61]. Additionally, Lin and Matzarakis reported diverse grades of thermal perception in a subtropical area, highlighting the adaptive comfort effect on human thermal perception across various climatic settings [62]. Thus, as shown in Table 3, the thermal sensations for different stress categories and PET values specific to Guangzhou were selected for this study. In this study, the PET output was obtained through the BIO-met module of ENVI-met. Considering that the main activity group comprised students, the characteristics of a standard person were set as a 19-year-old male, 1.71 m tall and 60.14 kg in weight [57,63], with a basic clothing insulation value of 0.4 clo. In addition, students mostly walk slowly in the outdoor spaces of the academic buildings; therefore, the metabolic rate was set to 2.0 met.

Table 3. Range for PET assessment in Guangzhou [57].

PET Value	Thermal Sensation	Grade of Physiological Stress
-	Very cold	Extreme cold stress
-	Cold	Strong cold stress
<11.3 °C	Cool	Moderate cold stress
11.3–19.2 °C	Slightly cool	Slight cold stress
19.2–24.6 °C	Comfortable	No thermal stress
24.6–29.1 °C	Slightly warm	Slight heat stress
29.1–36.3 °C	Warm	Moderate heat stress
36.3–53.6 °C	Hot	Strong heat stress
>53.6 °C	Very hot	Extreme heat stress

2.6. Estimation of the Sensible Heat Dynamic

An increase in sensible heat contributes to the warming of the atmosphere, which is the main cause of UHIs [64,65]. Evapotranspiration from vegetation, in combination with shading effects, can lower the ambient air temperature by a reduction in the sensible heat fluxes into the atmosphere. The energy savings from the cooling effect of green spaces can be estimated by measuring the sensible heat reduction; therefore, in this study, the sensible heat reduction of different tree species with different TCC scenarios was calculated using Equation (4) [66]:

$$\Delta E = C_p \cdot \Delta T \cdot \rho \cdot V \tag{4}$$

where ΔE is the energy variation (J), C_p is the specific heat of the air, which was set as 1.0×10^3 J/kg °C, ρ is the air density, which was set as 1.29 kg/m^3, ΔT is the air temperature difference between the two scenarios, and V is the air volume of different atmospheric layers.

Previous research on the thermal environment of courtyards has predominantly focused on the pedestrian-level thermal environment, which directly influences human thermal comfort [67–69]; however, the cooling effects of vegetation affect not only the near-surface thermal environmental layer but also extend to the higher atmospheric layers [66,70]. Therefore, to predict the effects of different TCCs on sensible heat reduction at various heights, the space was cut into seven layers according to the grid size in the Z-direction of the ENVI-met model, including 1.5 m, 2.1 m, 2.7 m, 4.5 m, 7.5 m, 11 m, and 14.5 m layers. In this study, the lower layers of the tree crown were situated at heights of 1.5 m, 2.1 m, and 2.7 m, while the upper layer of the tree crown was at a height of 14.5 m.

3. Results

3.1. Statistical Summary of the Thermal Environment and Model Accuracy Assessment

Table 4 shows the variation of T_a, T_g, RH and V_a at each measurement point. The average values of T_a and T_g at each measurement point were found to be greater than 32.6 °C. The RH ranged from 56.4% to 77.0%, and the average wind speed ranged from 0.3 m/s to 0.7 m/s. Thus, these climate conditions on the measurement days represent a typical summer climate in hot-humid areas.

Figure 2 displays the comparison between the simulated and measured air temperatures and RH values at each measured point. The R^2 between the measured and simulated values for T_a and RH were 0.88 and 0.94, respectively. The corresponding RMSE values ranged from 1.62 to 2.11 for the T_a and 2.62 to 3.73 for the RH, while the *MAE* ranged from 0.33 to 0.48 for the T_a and 0.41 to 0.63 for the RH. These values fall within the acceptable range based on previous studies, where *RMSE* values between 0.52 and 4.30 and *MAE* values between 0.27 and 3.67 have been considered acceptable [71,72]; therefore, the R^2, *RMSE* and *MAE* values obtained in this research indicate that the ENVI-met predictions in the context of this study were accurate enough. Regarding the air velocity, the software output value generally underestimated the air velocity level of the overhead layer [73]. Because the transitional space was ventilated on all sides, the actual wind field was subject to a large change in the wind speed and direction in real time. In addition to natural wind, the wind speed experienced by pedestrians in dynamic situations also includes the disturbance wind speed caused by walking [50]. Regarding the mean radiant temperature, wind speed is one of the main factors affecting the calculation of the mean radiant temperature, and the simulated differences in air velocity will lead to a difference in the mean radiant temperature. Although there are certain differences between the simulated and measured values, the changing trends in air velocity and mean radiant temperature can still reflect the impact of tree canopy coverage on the outdoor thermal environment.

Table 4. Statistical results of microclimate parameters.

Monitoring Points	Parameters	Minimum	Maximum	Mean	Standard Deviations
Point 1	T_a (°C)	29.3	33.9	32.7	1.19
	T_g (°C)	30.5	34.3	32.9	1.21
	RH (%)	58.7	76.0	65.5	5.39
	V_a (m/s)	0	1.5	0.4	0.39
Point 2	T_a (°C)	30.1	33.9	32.6	1.17
	T_g (°C)	30.4	34.1	32.8	1.10
	RH (%)	58.2	75.8	64.5	5.33
	V_a (m/s)	0	0.8	0.3	0.27
Point 3	T_a (°C)	30.0	33.9	32.6	1.25
	T_g (°C)	30.2	34.3	32.9	1.34
	RH (%)	57.9	77.0	64.8	5.68
	V_a (m/s)	0	2.2	0.6	0.47
Point 4	T_a (°C)	30.3	34.4	33.0	1.30
	T_g (°C)	28.8	34.5	32.9	1.68
	RH (%)	57.4	76.4	64.4	5.59
	V_a (m/s)	0	2.8	0.5	0.64
Point 5	T_a (°C)	30.1	34.3	32.8	1.34
	T_g (°C)	29.2	34.8	33.1	1.74
	RH (%)	56.4	76.3	63.9	5.80
	V_a (m/s)	0	1.7	0.7	0.55

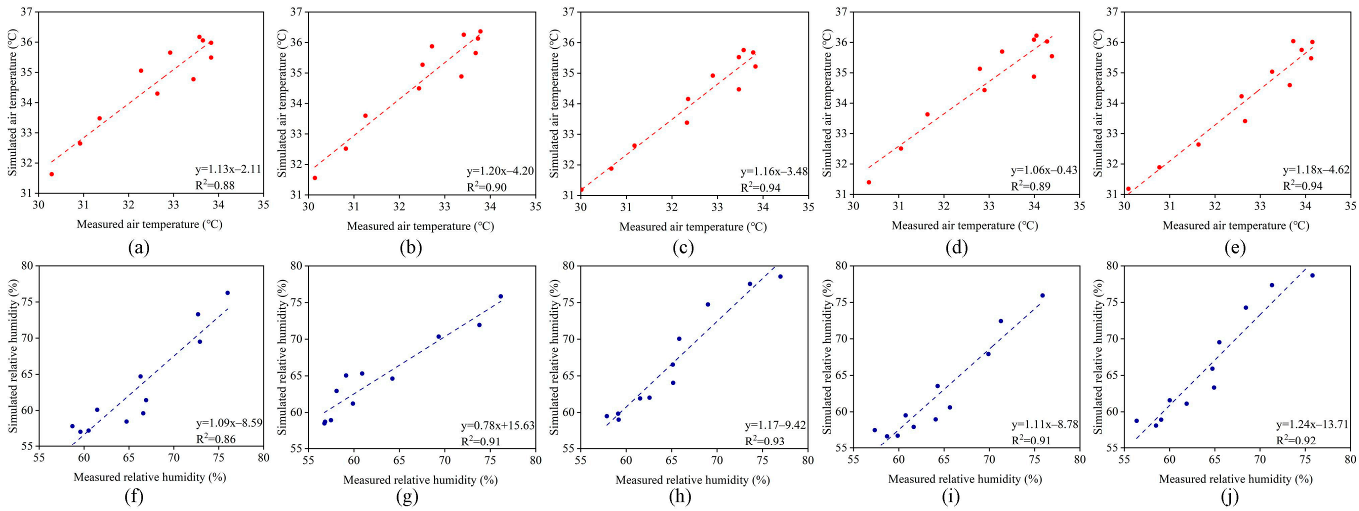

Figure 2. Correlation between the measured and simulated *Ta* and RH. (**a**–**e**) were *Ta* of point 1–5; (**f**–**j**) were RH of point 1–5.

3.2. Variation in T_a

Figure 3 illustrates the average T_a at a 1.5 m height of each courtyard with TCC from 0% to 68% at different times of the day. In the scenarios without trees (0% TCC), the T_a was higher in the DZXX between 8:00 a.m. and 13:00 p.m., and in the LX between 14:00 p.m. to 18:00 p.m., with the maximum T_a difference being 0.2 °C. This indicates that during the daytime, the T_a increased more slowly in the courtyards with higher H/W ratios than in those with lower H/W ratios. As the TCC increased, the T_a in each courtyard decreased, and scenarios with different TCCs simulated various cooling effects in courtyards with different H/W ratios. During the time period from 10:00 AM to 13:00 PM, the trees in the courtyard with a higher H/W ratio (LX) exhibited better cooling effects compared to the courtyard with a lower H/W ratio (DZXX). For example, when the TCC was 21%, there was essentially no reduction in the T_a in the DZXX; however, after 13:00 p.m., the temperature drop in the two courtyards became almost the same at the same TCC, with a difference of not more than 0.1 °C. When the TCC was 68%, the difference in the T_a between the two courtyards was 0.2 °C.

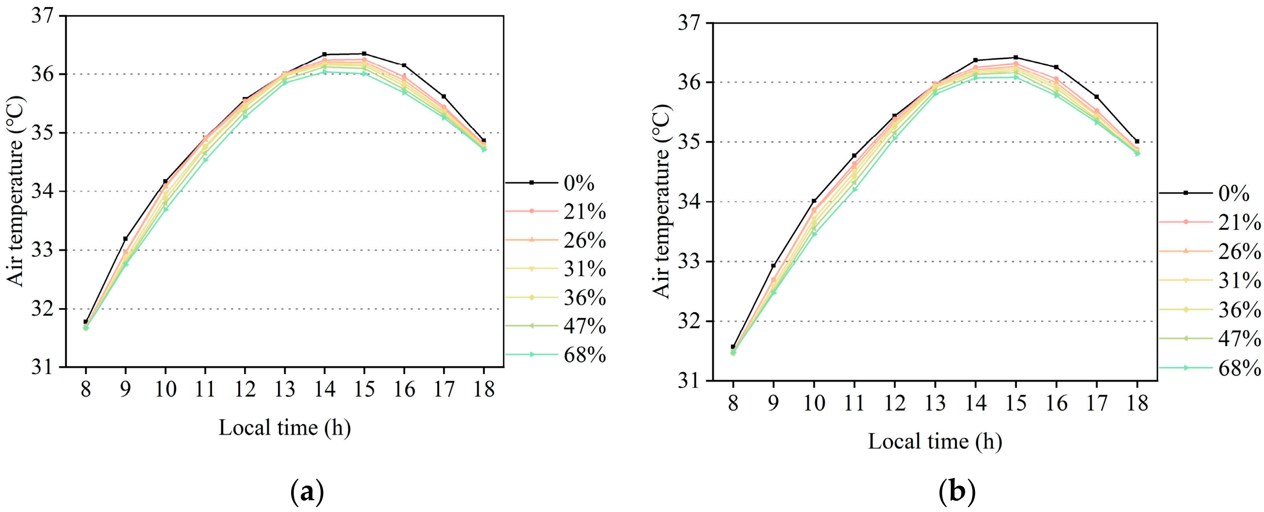

Figure 3. Average T_a at 1.5 m height of each courtyard with tree canopy cover from 0% to 68% at different times of the day. (**a**) DZXX and (**b**) LX.

3.3. Variation in T_{mrt}

Figure 4 shows the average T_{mrt} at a 1.5 m height of each courtyard with TCC from 0% to 68% at different times of the day. From 11:00 a.m. to 17:00 p.m., the average T_{mrt} values at a 1.5 m height in the LX were significantly higher than those in the DZXX, with the maximum difference in T_{mrt} between the two courtyards reaching up to 2.4 °C. As shown in Figure 5, the direct sun hours in the courtyards of the two academic buildings under typical summer conditions in hot-humid areas were simulated by using a Rhino's ladybug plugin (0% TCC). It is evident that the LX courtyard received more solar radiation than the DZXX under treeless conditions. As the TCC increased, the T_{mrt} values of each courtyard decreased substantially. The T_{mrt} values for each courtyard decreased the most when the TCC was 68%, by 10.6 °C and 10.7 °C, respectively. Furthermore, the maximum difference in the T_{mrt} between the two courtyards was reduced to 1.7 °C. This indicates that arranging trees can effectively reduce the differences in solar radiation between courtyards with different H/W ratios.

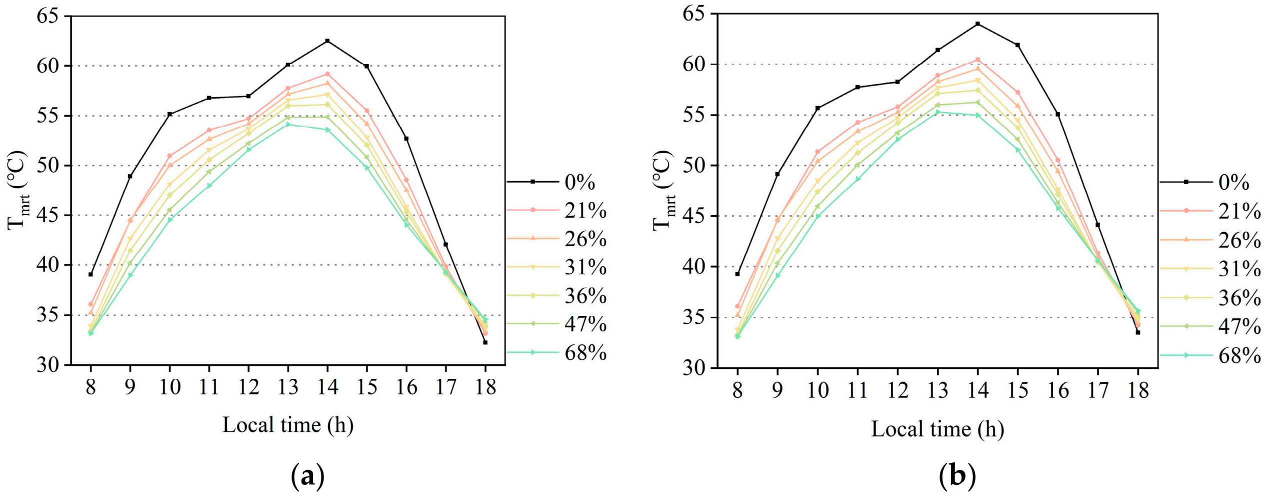

Figure 4. Average T_{mrt} at 1.5 m height of each courtyard with tree canopy cover from 0% to 68% at different times of the day. (**a**) DZXX and (**b**) LX.

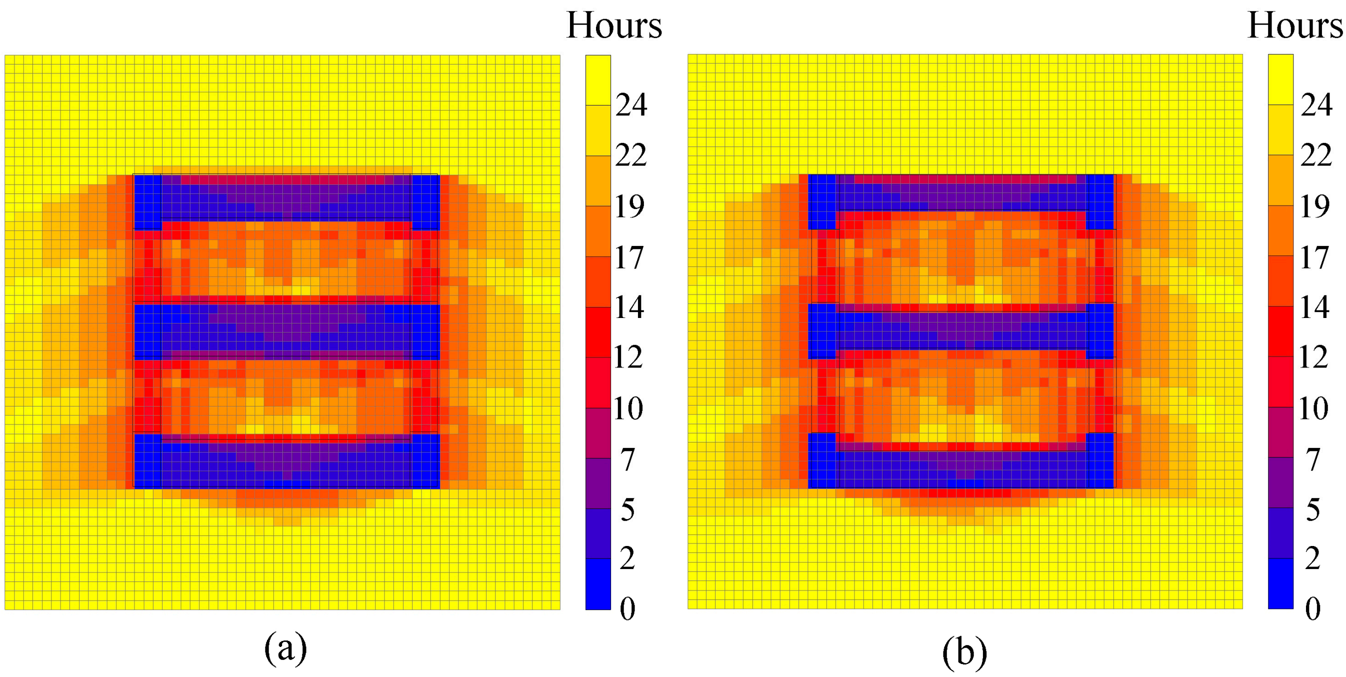

Figure 5. Direct sun hours of each courtyard (Daylight hour of the cases in a full day). (**a**) DZXX and (**b**) LX.

3.4. Thermal Comfort Assessment

The effects of different TCCs on the PET in different courtyards at each time period is shown in Figure 6. Based on the PET scale applied to Guangzhou, both courtyards made people feel "hot" at all times of the day under the treeless scenario. Compared to the courtyard of DZXX, the courtyard of LX had higher PET values, with a maximum difference of 0.7 °C at 16:00 p.m. Although arranging trees in each courtyard can reduce the PET values, the PET values in both courtyards remained at the "hot" level during each time period; however, as the TCC continued to rise to 68%, the PET values in each courtyard decreased by up to 5.4 °C (DZXX) and 5.5 °C (LX) at 9 a.m., respectively. This indicates that although planting trees can improve the outdoor thermal environment, it may be challenging to reduce the level of outdoor thermal comfort to a "warm" or lower category. Furthermore, at 14:00 p.m., which is the hottest time of the day, the difference in the PET between the two courtyards was only 0.2 °C (0% TCC); however, when the TCC was 68%, the PET difference between the two courtyards was 0.6 °C. This suggests that courtyards with a high H/W ratio combined with trees have a greater cooling effect than courtyards with a low H/W ratio.

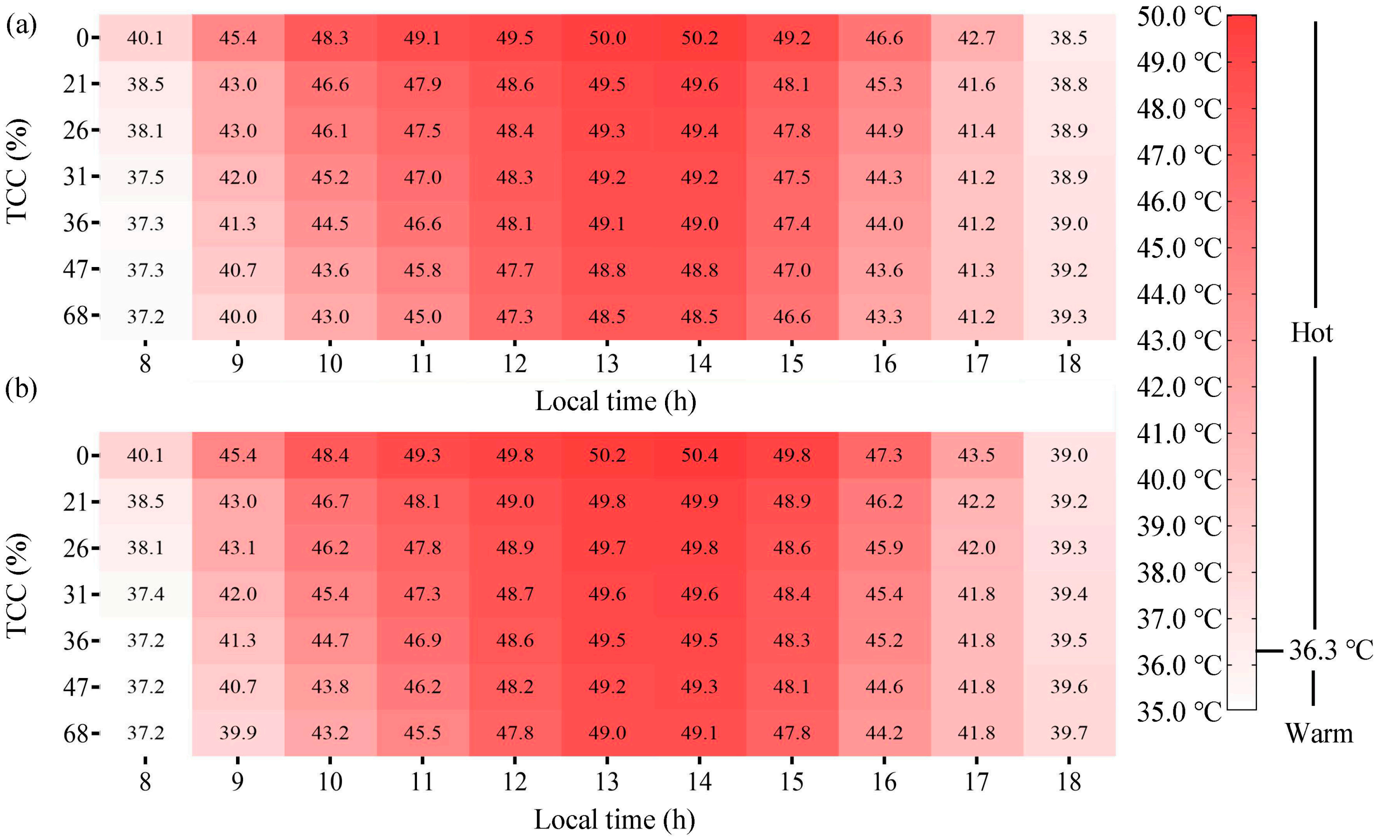

Figure 6. Average PET at 1.5 m height of each courtyard with tree canopy cover from 0% to 68% at different times of the day. (**a**) DZXX and (**b**) LX.

3.5. Sensible Heat Reduction

The results of a total sensible heat reduction for both courtyards, including all layers and time periods, are presented in Figure 7a,b. The total sensible heat reduction showed a significant and continuous increase with increasing the TCC in each courtyard. In the DZXX courtyard, the total sensible heat reductions for each TCC were 2.98×10^4 J/m^2 (21%), 3.64×10^4 J/m^2 (26%), 4.42×10^4 J/m^2 (31%), 4.98×10^4 J/m^2 (36%), 5.87×10^4 J/m^2 (47%), and 6.63×10^4 J/m^2 (68%), respectively. Similarly, in the courtyard of LX, the total sensible heat reductions for each TCC were 3.24×10^4 J/m^2 (21%), 3.92×10^4 J/m^2 (26%), 4.66×10^4 J/m^2 (31%), 5.30×10^4 J/m^2 (36%), 6.12×10^4 J/m^2 (47%), and 6.85×10^4 J/m^2 (68%), respectively. It is evident that when the TCC increased from 31% to 36%, the increase in the total sensible heat reduction in both courtyards decreased. Furthermore, Figure 7c,d show the percentage of the sensible heat reduction at different TCCs in the DZXX and LX courtyards for each height. As the TCC increased, the percentage of sensible heat reduction gradually increased at the lower levels (1.5–4.5 m) and decreased at the higher levels (11.0–14.5 m). This is because with the increase in the TCC, more trees were arranged in the center of the courtyard exposed to direct sunlight, resulting in a stronger cooling effect. However, due to the high level layer being more distance from the tree crown, the cooling ability of the tree canopy to that height is limited; therefore, the percentage of sensible heat reduction gradually decreased. In addition, the change in the percentage of sensible heat reduction in each level of the courtyards with low H/W ratios was more pronounced compared to that of the high H/W ratios.

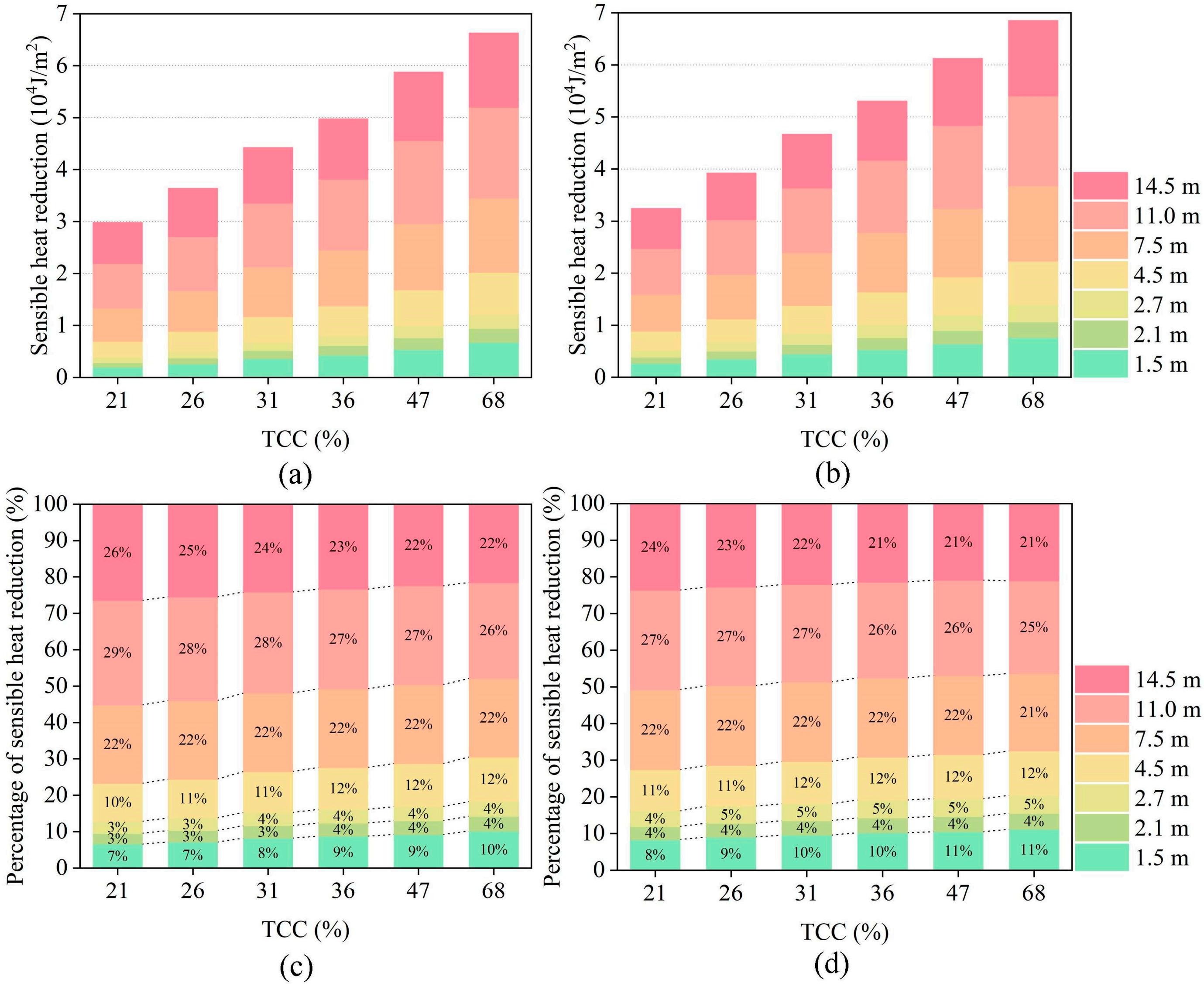

Figure 7. Reduction and percentage of sensible heat at different heights. (**a**) Sensible heat reduction of DZXX; (**b**) sensible heat reduction of LX; (**c**) percentage of sensible heat reduction at different heights in DZXX; (**d**) percentage of sensible heat reduction at different heights in LX.

4. Discussion

The influence of coverage of urban green spaces on mitigating the thermal environment has been widely recognized at the city to the neighborhood scale; however, few studies have focused on the cooling effects of vegetation at the courtyard scale [74–76]. In the present study, we analyzed the cooling effects of different TCCs in relation to courtyards with different H/W ratios. Consequently, trees planted in courtyards with high H/W ratios had a larger cooling effect during the hottest period of the day compared to courtyards with low H/W ratios. The results of this study were similar to the finding of Randa Mohamed Ahmed Mahmoud and Amr Sayed Hassan Abdallah, who investigated the effect of outdoor shading strategies on the thermal environment. They reported a higher influence of trees in shading a narrow courtyard with a H/W ratio of 0.7 compared to a wide courtyard with a H/W ratio of 0.4 [77]; however, it is worth noting that the academic buildings they surveyed were only 10 m high and enclosed on three sides, which could lead to different shadowing effects due to varying building heights and enclosure forms [41,78].

Moreover, Li et al. found that in residential areas with a building height of 33 m, a total sensible heat reduction of 7.08×10^4 J/m^2 was achieved with a 45% canopy coverage [70];

however, one of the findings of the present study is that the total sensible heat reduction for 47% TCC in courtyards with a high H/W ratio (0.9) was 5.87×10^4 J/m^2, while the total sensible heat reduction in courtyards with a low H/W ratio (0.7) was 6.12×10^4 J/m^2. This indicates that the lower the H/W ratio of a courtyard, the greater the sensible heat reduction achieved by planting trees. Additionally, when compared to outdoor open spaces, an increase in TCC in semi-outdoor spaces results in smaller cooling effects. This can be attributed to the higher percentage of building shadows in courtyards with higher H/W ratios. Furthermore, previous studies have also shown that trees located in building shadows have weaker cooling effects than those exposed to direct solar radiation [79–81]. In addition, It is essential to consider tree height as a significant factor affecting the reduction in sensible heat at different height layers; therefore, when planning green spaces in the built environment, the selection of tree species should take into account not only the leaf area index (LAI) value but also the tree height to optimize the cooling benefits.

This research does have certain limitations that should be acknowledged to better interpret the results. Firstly, the study assumed a uniform arrangement of trees in each courtyard, which may not represent the real-world diversity of tree distribution in courtyards. Future studies could consider more realistic scenarios with varied tree arrangements to better reflect the actual urban greenery patterns. Secondly, this study focused solely on the impact of tree canopy coverage on the thermal environment and sensible heat reduction during the summer season. As climate conditions and vegetation responses vary across different seasons, it would be beneficial to conduct further research exploring the cooling effects of different TCCs and tree species in various seasons throughout the year. Finally, from the perspective of site selection, our study only focused on two typical courtyards in Guangzhou. The cooling effect of trees also varies in cities located in different climates because the surface thermal fluxes are related to solar radiation [82]. Other types of courtyards should also be considered, because different dominant courtyard forms are found in different cities [83,84].

Despite these limitations, the study provides valuable insights into the cooling potential of the tree canopy coverage in academic building courtyards with different H/W ratios under hot-humid climate conditions. The findings contribute to the understanding of how urban green spaces can play a role in enhancing thermal comfort and mitigating urban heat island effects at the courtyard scale, which has been less explored in previous research.

5. Conclusions

This study presents the findings of an investigation into the impact of varying tree canopy coverage on the cooling of courtyards with different height-to-width (H/W) ratios, achieved by combining modeling with on-site measurements. The research was conducted in two similar academic buildings and their courtyard H/W ratios were 0.9 and 0.7. The results showed: (1) Arranging trees in courtyards with different H/W ratios has different effects, which produces variations in the microclimate. During the hottest period of the day, the PET value of courtyards with high H/W ratios decreases by up to 0.6 °C compared to courtyards with low H/W ratios. (2) Arranging trees in courtyards with different H/W ratios has different effects for sensible heat reduction. The maximum difference between the courtyards in this study with low H/W ratios and courtyards with high H/W ratios was 0.25×10^4 J/m^2. Some suggestions for good thermal environment in the local climate are:

1. Incorporate trees strategically: consider the strategic placement of trees in courtyards, particularly in courtyards with high H/W ratios, as they significantly contribute to cooling and improving microclimatic conditions.
2. Optimize tree canopy coverage: carefully select an appropriate percentage of tree canopy coverage to achieve the desired cooling effect, taking into account the specific conditions of each courtyard.
3. Select suitable tree species: in addition to considering the leaf area index (LAI) values, carefully choose tree species based on their height, as it significantly influences the sensible heat reduction at different height layers.

This study offers valuable insights into the distinct effects of trees on human thermal comfort and heat dynamics in courtyards of academic buildings with varying H/W ratios. These findings can be instrumental for university planners and designers in formulating comprehensive guidelines for courtyard design in academic buildings.

Author Contributions: Conceptualization, methodology, software, validation, formal analysis, investigation, and writing—original draft preparation, C.L. and J.Y.; writing—review and editing, C.L. and R.Z.; visualization, C.L.; supervision, C.L., J.H. and R.Z.; project administration, C.L., J.H. and R.Z.; funding acquisition, C.L. and R.Z. All authors have read and agreed to the published version of the manuscript.

Funding: This work is supported by the project "Research on Training Mode of Research Ability Involved in the Integration of Arts and Sciences" (grant no. 2021JGXM077), and "The research team for cross-disciplinary innovation and design at the intersection of art and technology" (grant no. 22TDD06).

Institutional Review Board Statement: Not applicable.

Informed Consent Statement: Not applicable.

Data Availability Statement: Not applicable.

Conflicts of Interest: The authors declare no conflict of interest.

References

1. Farhadi, H.; Faizi, M.; Sanaieian, H. Mitigating the urban heat island in a residential area in Tehran: Investigating the role of vegetation, materials, and orientation of buildings. *Sustain. Cities Soc.* **2019**, *46*, 101448. [CrossRef]
2. Kleerekoper, L.; van Esch, M.; Salcedo, T.B. How to make a city climate-proof, addressing the urban heat island effect. *Resour. Conserv. Recycl.* **2012**, *64*, 30–38. [CrossRef]
3. Gabriel, K.M.A.; Endlicher, W.R. Urban and rural mortality rates during heat waves in Berlin and Brandenburg, Germany. *Environ. Pollut.* **2011**, *159*, 2044–2050. [CrossRef] [PubMed]
4. McPhearson, T.; Mustafa, A.; Ortiz, L. Heat and COVID-19 could be twin killers. *Nature* **2020**, *582*, 32. [CrossRef]
5. Wang, Y.P.; Zacharias, J. Landscape modification for ambient environmental improvement in central business districts—A case from Beijing. *Urban For. Urban Green.* **2015**, *14*, 8–18. [CrossRef]
6. Luo, M.H.; Wang, Z.; Brager, G.; Cao, B.; Zhu, Y.X. Indoor climate experience, migration, and thermal comfort expectation in buildings. *Build. Environ.* **2018**, *141*, 262–272. [CrossRef]
7. Sarbu, I.; Sebarchievici, C. Aspects of indoor environmental quality assessment in buildings. *Energy Build.* **2013**, *60*, 410–419. [CrossRef]
8. Chen, Y.; Chen, B.; Lu, J.F. Influence of residential indoor environment on self-rated health in China: A cross-sectional study. *Sci. Technol. Built Environ.* **2022**, *28*, 916–927. [CrossRef]
9. Ding, Q.; Cai, W.J.; Wang, C.; Sanwal, M. The relationships between household consumption activities and energy consumption in china—An input-output analysis from the lifestyle perspective. *Appl. Energy* **2017**, *207*, 520–532. [CrossRef]
10. Niu, S.W.; Li, Z.; Qiu, X.; Dai, R.Q.; Wang, X.; Qiang, W.L.; Hong, Z.G. Measurement of effective energy consumption in China's rural household sector and policy implication. *Energy Policy* **2019**, *128*, 553–564. [CrossRef]
11. Aram, F.; Solgi, E.; Garcia, E.H.; Mosavi, A. Urban heat resilience at the time of global warming: Evaluating the impact of the urban parks on outdoor thermal comfort. *Environ. Sci. Eur.* **2020**, *32*, 117. [CrossRef]
12. Shooshtarian, S.; Lam, C.K.C.; Kenawy, I. Outdoor thermal comfort assessment: A review on thermal comfort research in Australia. *Build. Environ.* **2020**, *177*, 106917. [CrossRef]
13. Acero, J.A.; Koh, E.J.Y.; Ruefenacht, L.A.; Norford, L.K. Modelling the influence of high-rise urban geometry on outdoor thermal comfort in Singapore. *Urban Clim.* **2021**, *36*, 100775. [CrossRef]
14. Deng, J.Y.; Wong, N.H. Impact of urban canyon geometries on outdoor thermal comfort in central business districts. *Sustain. Cities Soc.* **2020**, *53*, 101966. [CrossRef]
15. Hwang, R.L.; Lin, T.P.; Matzarakis, A. Seasonal effects of urban street shading on long-term outdoor thermal comfort. *Build. Environ.* **2011**, *46*, 863–870. [CrossRef]
16. Lin, T.P.; Matzarakis, A.; Hwang, R.L. Shading effect on long-term outdoor thermal comfort. *Build. Environ.* **2010**, *45*, 213–221. [CrossRef]
17. Lin, B.R.; Li, X.F.; Zhu, Y.X.; Qin, Y.G. Numerical simulation studies of the different vegetation patterns' effects on outdoor pedestrian thermal comfort. *J. Wind Eng. Ind. Aerodyn.* **2008**, *96*, 1707–1718. [CrossRef]
18. Meili, N.; Acero, J.A.; Peleg, N.; Manoli, G.; Burlando, P.; Fatichi, S. Vegetation cover and plant-trait effects on outdoor thermal comfort in a tropical city. *Build. Environ.* **2021**, *195*, 107733. [CrossRef]

19. Taleghani, M.; Berardi, U. The effect of pavement characteristics on pedestrians' thermal comfort in Toronto. *Urban Clim.* **2018**, *24*, 449–459. [CrossRef]
20. Yuan, J.H.; Masuko, S.; Shimazaki, Y.; Yamanaka, T.; Kobayashi, T. Evaluation of outdoor thermal comfort under different building external-wall-surface with different reflective directional properties using CFD analysis and model experiment. *Build. Environ.* **2022**, *207*, 108478. [CrossRef]
21. Carpio, M.; Gonzalez, A.; Gonzalez, M.; Verichev, K. Influence of pavements on the urban heat island phenomenon: A scientific evolution analysis. *Energy Build.* **2020**, *226*, 110379. [CrossRef]
22. Zhu, J.Y.; Feng, J.J.; Lu, J.F.; Chen, Y.; Li, W.L.; Lian, P.J.; Zhao, X. A review of the influence of courtyard geometry and orientation on microclimate. *Build. Environ.* **2023**, *236*, 110269. [CrossRef]
23. Fang, Z.S.; He, H.Y.; Guo, Z.S.; Zheng, Z.M.; Feng, X.W. Daily variation of ground radiation in unshaded and shaded environments and the effect on mean radiant temperature. *Case Stud. Therm. Eng.* **2023**, *43*, 102791. [CrossRef]
24. Deng, J.Y.; He, Y.Y.; Dai, M.L. Evaluation of the outdoor thermal environment for three typical urban forms in Nanjing, China. *Build. Environ.* **2023**, *238*, 110358. [CrossRef]
25. Diz-Mellado, E.; Nikolopoulou, M.; Lopez-Cabeza, V.P.; Rivera-Gomez, C.; Galan-Marin, C. Cross-evaluation of thermal comfort in semi-outdoor spaces according to geometry in Southern Spain. *Urban Clim.* **2023**, *49*, 101491. [CrossRef]
26. Diz-Mellado, E.; Ruiz-Pardo, A.; Rivera-Gomez, C.; de la Flor, F.J.S.; Galan-Marin, C. Unravelling the impact of courtyard geometry on cooling energy consumption in buildings. *Build. Environ.* **2023**, *237*, 110349. [CrossRef]
27. Nasrollahi, N.; Hatami, M.; Khastar, S.R.; Taleghani, M. Numerical evaluation of thermal comfort in traditional courtyards to develop new microclimate design in a hot and dry climate. *Sustain. Cities Soc.* **2017**, *35*, 449–467. [CrossRef]
28. Rodriguez-Algeciras, J.; Tablada, A.; Chaos-Yeras, M.; De la Paz, G.; Matzarakis, A. Influence of aspect ratio and orientation on large courtyard thermal conditions in the historical centre of Camaguey-Cuba. *Renew. Energy* **2018**, *125*, 840–856. [CrossRef]
29. Jin, Y.; Yoon, H. Evaluating planting strategies for outdoor thermal comfort in high-rise residential complexes: A computational fluid dynamics simulation study. *Environ. Sci. Pollut. Res. Int.* **2023**, *30*, 88641–88663. [CrossRef]
30. Zhao, Q.S.; Sailor, D.J.; Wentz, E.A. Impact of tree locations and arrangements on outdoor microclimates and human thermal comfort in an urban residential environment. *Urban For. Urban Green.* **2018**, *32*, 81–91. [CrossRef]
31. Zhang, A.X.; Bokel, R.; van den Dobbelsteen, A.; Sun, Y.C.; Huang, Q.; Zhang, Q. An integrated school and schoolyard design method for summer thermal comfort and energy efficiency in Northern China. *Build. Environ.* **2017**, *124*, 369–387. [CrossRef]
32. Yu, Z.W.; Chen, T.T.; Yang, G.Y.; Sun, R.H.; Xie, W.; Vejre, H. Quantifying seasonal and diurnal contributions of urban landscapes to heat energy dynamics. *Appl. Energy* **2020**, *264*, 114724. [CrossRef]
33. Li, X.X.; Liu, X. Effect of tree evapotranspiration and hydrological processes on urban microclimate in a tropical city: A WRF/SLUCM study. *Urban Clim.* **2021**, *40*, 101009. [CrossRef]
34. Heusinger, J.; Sailor, D.J.; Weber, S. Modeling the reduction of urban excess heat by green roofs with respect to different irrigation scenarios. *Build. Environ.* **2018**, *131*, 174–183. [CrossRef]
35. Ali-Toudert, F. Exploration of the thermal behaviour and energy balance of urban canyons in relation to their geometrical and constructive properties. *Build. Environ.* **2021**, *188*, 107466. [CrossRef]
36. Marciotto, E.R.; Oliveira, A.P.; Hanna, S.R. Modeling study of the aspect ratio influence on urban canopy energy fluxes with a modified wall-canyon energy budget scheme. *Build. Environ.* **2010**, *45*, 2497–2505. [CrossRef]
37. Salata, F.; Golasi, L.; Volloaro, R.D.; Vollaro, A.D. Urban microclimate and outdoor thermal comfort. A proper procedure to fit ENVI-met simulation outputs to experimental data. *Sustain. Cities Soc.* **2016**, *26*, 318–343. [CrossRef]
38. Tsoka, S.; Tsikaloudaki, A.; Theodosiou, T. Analyzing the ENVI-met microclimate model's performance and assessing cool materials and urban vegetation applications—A review. *Sustain. Cities Soc.* **2018**, *43*, 55–76. [CrossRef]
39. Yin, S.; Lang, W.; Xiao, Y.Q. The synergistic effect of street canyons and neighbourhood layout design on pedestrian-level thermal comfort in hot-humid area of China. *Sustain. Cities Soc.* **2019**, *49*, 101571. [CrossRef]
40. Yin, S.; Wang, F.; Xiao, Y.Q.; Xue, S.H. Comparing cooling efficiency of shading strategies for pedestrian thermal comfort in street canyons of traditional shophouse neighbourhoods in Guangzhou, China. *Urban Clim.* **2022**, *43*, 101165. [CrossRef]
41. Lopez-Cabeza, V.P.; Galan-Marin, C.; Rivera-Gomez, C.; Roa-Fernandez, J. Courtyard microclimate ENVI-met outputs deviation from the experimental data. *Build. Environ.* **2018**, *144*, 129–141. [CrossRef]
42. Yilmaz, S.; Mutlu, E.; Yilmaz, H. Alternative scenarios for ecological urbanizations using ENVI-met model. *Environ. Sci. Pollut. Res.* **2018**, *25*, 26307–26321. [CrossRef] [PubMed]
43. Li, K.M.; Zhang, Y.F.; Zhao, L.H. Outdoor thermal comfort and activities in the urban residential community in a humid subtropical area of China. *Energy Build.* **2016**, *133*, 498–511. [CrossRef]
44. Alfano, F.R.D.; Dell'Isola, M.; Ficco, G.; Palella, B.I.; Riccio, G. Small globes and pocket heat stress meters for WBGT and PHS evaluations. A critical analysis under controlled conditions. *Build. Environ.* **2022**, *226*, 109781. [CrossRef]
45. Alfano, F.R.D.; Ficco, G.; Frattolillo, A.; Palella, B.I.; Riccio, G. Mean Radiant Temperature Measurements through Small Black Globes under Forced Convection Conditions. *Atmosphere* **2021**, *12*, 621. [CrossRef]
46. Yang, J.H.; Zhao, Y.; Guo, T.Y.; Luo, X.Y.; Ji, K.F.; Zhou, M.; Wan, F.D. The impact of tree species and planting location on outdoor thermal comfort of a semi-outdoor space. *Int. J. Biometeorol.* **2023**, *67*, 1689–1701. [CrossRef]

47. Liu, Z.X.; Cheng, W.W.; Jim, C.Y.; Morakinyo, T.E.; Shi, Y.; Ng, E. Heat mitigation benefits of urban green and blue infrastructures: A systematic review of modeling techniques, validation and scenario simulation in ENVI-met V4. *Build. Environ.* **2021**, *200*, 107939. [CrossRef]
48. Aboelata, A.; Sodoudi, S. Evaluating the effect of trees on UHI mitigation and reduction of energy usage in different built up areas in Cairo. *Build. Environ.* **2020**, *168*, 106490. [CrossRef]
49. Susca, T.; Zanghirella, F.; Del Fatto, V. Building integrated vegetation effect on micro-climate conditions for urban heat island adaptation. Lesson learned from Turin and Rome case studies. *Energy Build.* **2023**, *295*, 113233. [CrossRef]
50. Zhang, Y.C.; Lin, Z.; Fang, Z.S.; Zheng, Z.M. An improved algorithm of thermal index models based on ENVI-met. *Urban Clim.* **2022**, *44*, 101190. [CrossRef]
51. Calasan, M.; Aleem, S.; Zobaa, A.F. On the root mean square error (RMSE) calculation for parameter estimation of photovoltaic models: A novel exact analytical solution based on Lambert W function. *Energy Convers. Manag.* **2020**, *210*, 112716. [CrossRef]
52. Liu, Z.X.; Brown, R.D.; Zheng, S.L.; Jiang, Y.; Zhao, L.H. An in-depth analysis of the effect of trees on human energy fluxes. *Urban For. Urban Green.* **2020**, *50*, 126646. [CrossRef]
53. Huang, B.Z.; Hong, B.; Tian, Y.; Yuan, T.T.; Su, M.F. Outdoor thermal benchmarks and thermal safety for children: A study in China's cold region. *Sci. Total Environ.* **2021**, *787*, 147603. [CrossRef]
54. Tang, T.W.; Zhou, X.Q.; Zhang, Y.C.; Feng, X.W.; Liu, W.W.; Fang, Z.S.; Zheng, Z.M. Investigation into the thermal comfort and physiological adaptability of outdoor physical training in college students. *Sci. Total Environ.* **2022**, *839*, 155979. [CrossRef]
55. Elnabawi, M.H.; Hamza, N.; Dudek, S. Thermal perception of outdoor urban spaces in the hot arid region of Cairo, Egypt. *Sustain. Cities Soc.* **2016**, *22*, 136–145. [CrossRef]
56. Hoppe, P. The physiological equivalent temperature—A universal index for the biometeorological assessment of the thermal environment. *Int. J. Biometeorol.* **1999**, *43*, 71–75. [CrossRef]
57. Fang, Z.S.; Feng, X.W.; Xu, X.N.; Zhou, X.Q.; Lin, Z.; Ji, Y. Investigation into outdoor thermal comfort conditions by different seasonal field surveys in China, Guangzhou. *Int. J. Biometeorol.* **2019**, *63*, 1357–1368. [CrossRef]
58. Abdallah, A.S.H.; Mahmoud, R.M.A. Urban morphology as an adaptation strategy to improve outdoor thermal comfort in urban residential community of new assiut city, Egypt. *Sustain. Cities Soc.* **2022**, *78*, 103648. [CrossRef]
59. Lam, C.K.C.; Lee, H.; Yang, S.R.; Park, S. A review on the significance and perspective of the numerical simulations of outdoor thermal environment. *Sustain. Cities Soc.* **2021**, *71*, 102971. [CrossRef]
60. Lan, H.N.; Lau, K.K.L.; Shi, Y.; Ren, C. Improved urban heat island mitigation using bioclimatic redevelopment along an urban waterfront at Victoria Dockside, Hong Kong. *Sustain. Cities Soc.* **2021**, *74*, 103172. [CrossRef]
61. Lai, D.Y.; Guo, D.H.; Hou, Y.F.; Lin, C.Y.; Chen, Q.Y. Studies of outdoor thermal comfort in northern China. *Build. Environ.* **2014**, *77*, 110–118. [CrossRef]
62. Lin, T.P.; Matzarakis, A. Tourism climate and thermal comfort in Sun Moon Lake, Taiwan. *Int. J. Biometeorol.* **2008**, *52*, 281–290. [CrossRef] [PubMed]
63. Fang, Z.S.; Xu, X.N.; Zhou, X.Q.; Deng, S.Q.; Wu, H.J.; Liu, J.L.; Lin, Z. Investigation into the thermal comfort of university students conducting outdoor training. *Build. Environ.* **2019**, *149*, 26–38. [CrossRef]
64. Arnfield, A.J. Two decades of urban climate research: A review of turbulence, exchanges of energy and water, and the urban heat island. *Int. J. Climatol.* **2003**, *23*, 1–26. [CrossRef]
65. Hu, Y.H.; Hou, M.T.; Jia, G.S.; Zhao, C.L.; Zhen, X.J.; Xu, Y.H. Comparison of surface and canopy urban heat islands within megacities of eastern China. *Isprs J. Photogramm. Remote Sens.* **2019**, *156*, 160–168. [CrossRef]
66. Wu, Z.F.; Chen, L.D. Optimizing the spatial arrangement of trees in residential neighborhoods for better cooling effects: Integrating modeling with in-situ measurements. *Landsc. Urban Plan.* **2017**, *167*, 463–472. [CrossRef]
67. Abdallah, A.S.H. Passive design strategies to improve student thermal comfort in Assiut University: A field study in the Faculty of Physical Education in hot season. *Sustain. Cities Soc.* **2022**, *86*, 104110. [CrossRef]
68. Elgheznawy, D.; Eltarabily, S. The impact of sun sail-shading strategy on the thermal comfort in school courtyards. *Build. Environ.* **2021**, *202*, 108046. [CrossRef]
69. Lopez-Cabeza, V.P.; Alzate-Gaviria, S.; Diz-Mellado, E.; Rivera-Gomez, C.; Galan-Marin, C. Albedo influence on the microclimate and thermal comfort of courtyards under Mediterranean hot summer climate conditions. *Sustain. Cities Soc.* **2022**, *81*, 103872. [CrossRef]
70. Li, Y.N.; Lin, D.L.; Zhang, Y.H.; Song, Z.P.; Sha, X.H.; Zhou, S.Q.; Chen, C.; Yu, Z.W. Quantifying tree canopy coverage threshold of typical residential quarters considering human thermal comfort and heat dynamics under extreme heat. *Build. Environ.* **2023**, *233*, 110100. [CrossRef]
71. Li, J.Y.; Zheng, B.H.; Bedra, K.B. Evaluating the improvements of thermal comfort by different natural elements within courtyards in Singapore. *Urban Clim.* **2022**, *45*, 101253. [CrossRef]
72. Salata, F.; Golasi, L.; Petitti, D.; Vollaro, E.D.L.; Coppi, M.; Vollaro, A.D.L. Relating microclimate, human thermal comfort and health during heat waves: An analysis of heat island mitigation strategies through a case study in an urban outdoor environment. *Sustain. Cities Soc.* **2017**, *30*, 79–96. [CrossRef]
73. Crank, P.J.; Sailor, D.J.; Ban-Weiss, G.; Taleghani, M. Evaluating the ENVI-met microscale model for suitability in analysis of targeted urban heat mitigation strategies. *Urban Clim.* **2018**, *26*, 188–197. [CrossRef]

74. Fahmy, M.; Mahdy, M.; Mahmoud, S.; Abdelalim, M.; Ezzeldin, S.; Attia, S. Influence of urban canopy green coverage and future climate change scenarios on energy consumption of new sub-urban residential developments using coupled simulation techniques: A case study in Alexandria, Egypt. *Energy Rep.* **2020**, *6*, 638–645. [CrossRef]
75. Kim, S.W.; Brown, R.D.; Winslow, J.F. Urban green and blue infrastructure effect on the micro-scale thermal environment in a residential neighborhood: Mueller, Austin, TX. *Int. J. Sustain. Dev. World Ecol.* **2023**, 1–15. [CrossRef]
76. Shashua-Bar, L.; Tsiros, I.X.; Hoffman, M. Passive cooling design options to ameliorate thermal comfort in urban streets of a Mediterranean climate (Athens) under hot summer conditions. *Build. Environ.* **2012**, *57*, 110–119. [CrossRef]
77. Mahmoud, R.M.A.; Abdallah, A.S.H. Assessment of outdoor shading strategies to improve outdoor thermal comfort in school courtyards in hot and arid climates. *Sustain. Cities Soc.* **2022**, *86*, 104147. [CrossRef]
78. Forouzandeh, A. Numerical modeling validation for the microclimate thermal condition of semi-closed courtyard spaces between buildings. *Sustain. Cities Soc.* **2018**, *36*, 327–345. [CrossRef]
79. Feng, L.; Yang, S.Q.; Zhou, Y.N.; Shuai, L.R. Exploring the effects of the spatial arrangement and leaf area density of trees on building wall temperature. *Build. Environ.* **2021**, *205*, 108295. [CrossRef]
80. Hong, B.; Lin, B.R. Numerical studies of the outdoor wind environment and thermal comfort at pedestrian level in housing blocks with different building layout patterns and trees arrangement. *Renew. Energy* **2015**, *73*, 18–27. [CrossRef]
81. Zhao, Y.F.; Chen, Y.H.; Li, K.N. A simulation study on the effects of tree height variations on the facade temperature of enclosed courtyard in North China. *Build. Environ.* **2022**, *207*, 108566. [CrossRef]
82. Shi, Y.R.; Xiang, Y.R.; Zhang, Y.F. Urban Design Factors Influencing Surface Urban Heat Island in the High-Density City of Guangzhou Based on the Local Climate Zone. *Sensors* **2019**, *19*, 3459. [CrossRef]
83. Berkovic, S.; Yezioro, A.; Bitan, A. Study of thermal comfort in courtyards in a hot arid climate. *Sol. Energy* **2012**, *86*, 1173–1186. [CrossRef]
84. Alkhoudiri, A.; Navarro, I.; Fort, J.M.; Alumran, S. Parametric comparative analysis of outdoor thermal comfort in a desert climate: A case study of single-family houses in Riyadh. *Urban Clim.* **2022**, *46*, 101300. [CrossRef]